ResearchGate

See discussions, stats, and author profiles for this publication at: https://www.researchgate.net/publication/236956157

Theoretical Analysis of the Influence of Chelate-Ring Size and Vicinal Effects on Electronic Circular Dichroism Spectra of Cobalt(III) EDDA-Type Complexes

ARTICLE *in* THE JOURNAL OF PHYSICAL CHEMISTRY A · MAY 2013

Impact Factor: 2.69 · DOI: 10.1021/jp403145h · Source: PubMed

CITATIONS
2

READS
34

6 AUTHORS, INCLUDING:

Yuekui Wang
Shanxi University
27 PUBLICATIONS **397** CITATIONS

SEE PROFILE

Available from: Yuekui Wang
Retrieved on: 26 January 2016

THE JOURNAL OF PHYSICAL CHEMISTRY A

Article

pubs.acs.org/JPCA

Theoretical Analysis of the Influence of Chelate-Ring Size and Vicinal Effects on Electronic Circular Dichroism Spectra of Cobalt(III) EDDA-Type Complexes

Ai Wang, Yuekui Wang,* Jie Jia, Lixia Feng, Chunxia Zhang, and Linlin Liu

Key Laboratory of Chemical Biology and Molecular Engineering of the Education Ministry, Institute of Molecular Science, Shanxi University, Taiyuan, Shanxi 030006, P. R. China

Supporting Information

ABSTRACT: To assess the contributions of configurational and vicinal effects as well as chelate-ring size to rotational strengths, the geometries of a series of cobalt(III) complexes [Co(EDDA-type)(L)]$^{\pm}$ with the tetradentate EDDA-type ligands, EDDA (ethylenediamine-*N*,*N*′-diacetate), DMEDDA (*N*,*N*′-dimethylethylenediamine-*N*,*N*′-diacetate), DEEDDA (*N*,*N*′-diethylethylenediamine-*N*,*N*′-diacetate), and a bidentate ancillary ligand L (L = ethylenediamine, oxalate, carbonate, (*S*)-alanine, and malonate) in aqueous solution have been optimized at the DFT/B3LYP/6-311++G(2d,p) level of theory. Based on the optimized geometries, the excitation energies and oscillator and rotational strengths have been calculated using the time-dependent density functional theory (TDDFT) method with the same functional and basis set. The calculated circular dichroism (CD) curves are in excellent agreement with the observed ones except for some small red or blue shifts in peak wavelengths. For the influence of chelate-ring size of the bidentate ligands on the CD intensities, a qualitative analysis together with the quantitative TDDFT calculation reveal that it depends on the symmetry of the cobalt-EDDA backbone. For the *s-cis*-isomers, the influence is negligible due to the perturbation is symmetric. For the *uns-cis*-isomers, the perturbation is unsymmetric. Since a small ring size means a large perturbation, this leads to the integral CD intensities decreasing with increasing the chelate ring size. The vicinal effects of asymmetric nitrogens incorporate both the substitutent effects and conformational relaxation effects, with the former being dominant. By analyzing the contributions of chiral arrays to rotational strengths, we found that the part of contributions dominated by the *S*-type chiral nitrogens could be considered as a good measure for the vicinal effects of chiral nitrogens. In addition, we found that the twist form (δ/λ) of the backbone ethylenediamine ring (E-ring) of the coordinated EDDA-type ligands is a key factor to understand the properties of these chelates, because it not only dominates the relative stabilities of the *s-cis*-Λ(*SS*)-diastereoisomers with the result that $\lambda > \delta$ but also affects the major CD band by changing the order of the first two transitions. Moreover, the twist angle of E-ring is inversely related to the vicinal effect of chiral nitrogens. These findings may help us to understand the chelate ring size as well as vicinal effect related chiroptical phenomenon of the cobalt EDDA-type chelates.

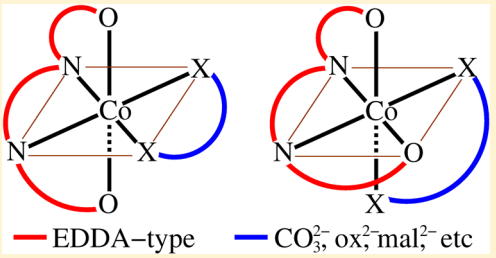

INTRODUCTION

Since some cobalt(III) chelates of ethylenediamine-*N*,*N*′-diacetic acid (H_2EDDA) were first reported[1] by Mori et al. in 1962, investigations of chiral coordination compounds with EDDA and related ligands have received much attention due to the good chelating ability of the ligands, which usually act as electron donors and can promise a variety of stereochemical and physical properties for the corresponding complexes.

Thereafter, a great number of transition metal complexes with EDDA and related ligands have been isolated,[2] and some of them have been also well-characterized using different methods, including X-ray[3,4] diffraction, spectroscopic (IR, Raman, NMR, ESR, UV−vis, and CD)[5] techniques, electrochemistry,[6] kinetic and thermodynamic information,[7,8] hydrolysis phenomena,[9] as well as condensation reactions.[10] Nowadays, they have given rise to a wide range of applications in chemistry,[2] biology,[11,12] and medicine.[13,14]

Among these complexes, the octahedral cobalt(III) chelates[15,16] [Co(EDDA-type)(L)]$^{\pm}$ containing one of the tetradentate dianion ligands, EDDA (ethylenediamine-*N*,*N*′-diacetate), DMEDDA (*N*,*N*′-dimethylethylenediamine-*N*,*N*′-diacetate), DEEDDA (*N*,*N*′-diethylethylenediamine-*N*,*N*′-diacetate), and a bidentate ancillary ligand L are of particular interest, because they have played a prominent role as model systems in the stereochemical study of transition metal complexes.

As far as the chiroptical properties and stereochemistry of these cobalt(III) chelates are concerned, much work has been done both experimentally[2,5] and theoretically[17,18] during the past five decades. Considerable progress has been made in correlating the observed electronic circular dichroism (ECD)

Received: March 30, 2013
Revised: May 17, 2013
Published: May 28, 2013

ACS Publications © 2013 American Chemical Society

dx.doi.org/10.1021/jp403145h | J. Phys. Chem. A 2013, 117, 5061−5072

and optical rotatory dispersion (ORD) spectra with specific stereochemical features of the series complexes. However, there remain some interesting experimental phenomena which are not yet well understood, due in large part to a lack of high-level theoretical analyses, especially at the first-principle level. For example, by comparison of the ECD spectra of the cobalt(III) complexes $[Co(EDDA)(L)]^-$, where L is respectively the bidentate ligand carbonate (CO_3^{2-}), oxalate (ox^{2-}), malonate (mal^{2-}), ethylenediamine (en), and *S*-alanine ((*S*)-ala$^-$), Van Saun and Douglas[19] found that rotational strengths of the d−d transitions are determined largely by the EDDA backbone and quite insensitive to the bidentate ligand L used; later Jordan and Legg[20] pointed out that the net rotational strengths for the dianion series exhibit a tendency to decrease in the order $CO_3^{2-} > ox^{2-} > mal^{2-}$, with increasing the chelate ring size. For chelates with different EDDA-type ligands, the contribution from the chiral nitrogen atoms in coordinated EDDA to the rotational strength of the first CD band was found[21−23] to be much greater than those in DMEDDA and DEEDDA. Here, the latter effect may be explained by the vicinal effect of chiral nitrogen donor atoms in terms of the crystal field theory[18] (CFT), but the former effect and related problems cannot be understood at this level of theory. In fact, both effects are dependent upon the configurations of complexes, and therefore, more rigorous theoretical work on the origin of rotational strengths in these systems is needed to get a deep insight to the phenomena.

In recent years, with the development of density functional theory (DFT) and especially the improvement of time-dependent density functional theory (TDDFT),[24] properties of both ground- and excited-states for medium-sized metal complexes can be calculated at the first-principle level with good accuracy.[25,26] This makes it possible to perform such an analysis for the chelates.

In this paper, we shall present and discuss calculations of the series cobalt(III) chelates $[Co(EDDA\text{-type})(L)]^{\pm}$ (L = en, ox^{2-}, mal^{2-}, CO_3^{2-}, and *S*-ala$^-$) at the first-principle level. The main object of this research is to clarify the relationship between the chiroptical properties and stereochemical features of the complexes and to quantitatively assess the individual contributions of various sterically chiral arrangements to the CD spectra, including the *N*-vicinal effects and chelate ring size effects, and so forth. The computational details are summarized in the next section. Analyses and discussions on the results are presented in section 3. Finally, the main conclusions and findings are given in section 4.

COMPUTATIONAL DETAILS

In the mixed-ligand cobalt(III) complexes $[Co(EDDA\text{-type})(L)]^{\pm}$, the linear flexible tetradentate EDDA-type ligand can occupy four of the octahedral sites around the metal ion to form the three possible geometrical isomers[5] (with respect to the coordinated atoms X), symmetrical *cis* (*s-cis*), unsymmetrical *cis* (*uns-cis*), and *trans*, as shown in Figure 1. However, for the bidentate ligands L mentioned above, only the *s-cis* and *uns-cis* isomers are possible due to the limited size of L, with the *s-cis* form being naturally favored.[2] In this form, the complex possesses two out-of-plane glycinate (G) rings and the backbone ethylenediamine (E) ring.

Since the complexes incorporate four nonplanar five-membered chelate rings in a propeller-like disposition and display both configurational and conformational chirality, that is, Δ/Λ at the octahedral core, *R*/*S* at the nitrogen atoms of

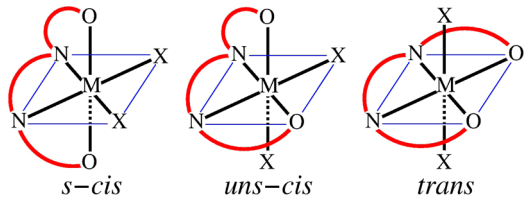

Figure 1. Three possible geometrical isomers of six-coordinate complexes possessing a tetradentate EDDA-type ligand.

EDDA-type ligand, and δ/λ twists of the chelate rings, their absolute configurations can be clearly specified by combining these chirality notations, as depicted in Figure 2. The grouped

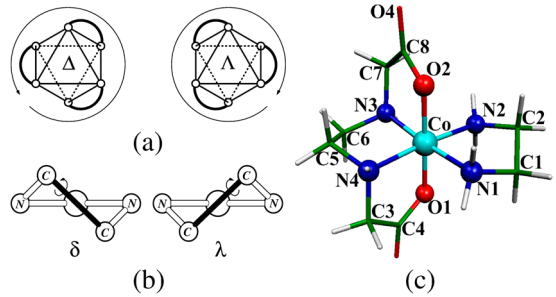

Figure 2. (a) The Δ/Λ octahedral core; (b) δ/λ twists of five-membered chelate ring; (c) absolute configuration of *s-cis*-$C_2\Lambda(SS)$-$(\delta\lambda\delta)(\lambda)[Co(EDDA)(en)]^+$ complex.

notation $C_2\Lambda(SS)(\delta\lambda\delta)(\lambda)$ means that the $[Co(EDDA)(en)]^+$ complex is of C_2-symmetry and characterized by a Λ-octahedral core, two (*S*)-type chiral nitrogens on the EDDA ligand whose chelate rings (GEG) exhibit a twist pattern of $(\delta\lambda\delta)$, and one (λ)-twisted en ligand, respectively.

Since the CD spectra of each pair of enantiomers have the same magnitude but are opposite in sign, calculations will be restricted to the Λ-configuration only, as the CD of the Δ-enantiomer can be generated simply by a mirror operation.

Initial geometries of the 24 Λ-diastereoisomers of chelates $[Co(EDDA\text{-type})(L)]^{\pm}$ (L = en, ox^{2-}) and $[Co(EDDA)(L)]^{0/-}$ (L = CO_3^{2-}, (*S*)-ala$^-$, mal^{2-}) were constructed by referring to the X-ray structure[4] of *s-cis*-$[Co(EDDA)(en)]ClO_4$. The ground-state geometry optimizations and subsequent frequency calculations were performed employing the DFT method, as implemented in Gaussian09 program package,[27] with the B3LYP hybrid functional[28] and 6-311++G(2d,p) basis set. The excitation energies, oscillator, and rotational strengths of the 60 lowest-lying singlet excited states for the optimized geometries were then calculated using the TDDFT method with the same functional and basis set. In all cases, solvent (water) effects have been included using the polarizable continuum model (PCM)[29] in the integral equation formalism (IEF).

RESULTS AND DISCUSSIONS

Optimized Geometry Parameters. The optimized geometries of the 24 stable Λ-diastereoisomers are displayed in Figure S1 (see Supporting Information), and some of the most stable structures with different bidentate ligands are depicted in Figure 3. A short comparison between the optimized and observed bond parameters for $C_2\Lambda(SS)(\delta\lambda\delta)(\lambda)[Co(EDDA)(en)]^+$ is given in Table 1. Since the calculated values are for single molecules in solution, not for that in crystal, the

dx.doi.org/10.1021/jp403145h | J. Phys. Chem. A 2013, 117, 5061−5072

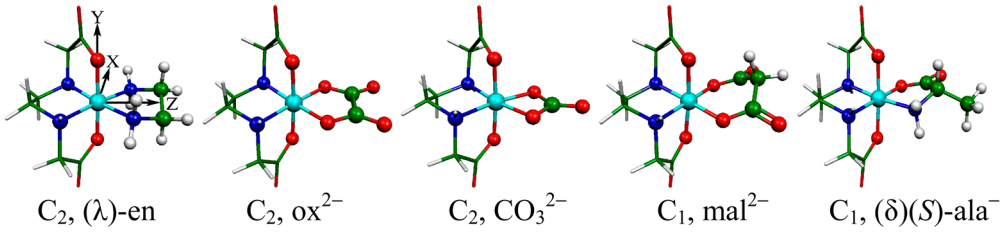

Figure 3. Optimized geometries of $\Lambda(SS)(\delta\lambda\delta)(\lambda)[Co(EDDA)(L)]^{\pm}$ complexes with L = (λ)-en, ox^{2-}, CO_3^{2-}, mal^{2-}, and $(\delta)(S)$-ala^-. The coordinate system is shown in the first structure.

agreement between the optimized and observed parameters is clearly acceptable.

Table 1. Comparison of the Calculated and Observed Structural Parameters of *s-cis*-$C_2\Lambda(SS)(\delta\lambda\delta)(\lambda)$[Co(EDDA)-(en)]$^+$ Isomer[a]

parameter	calcd	X-ray[4]	parameter	calcd	X-ray[4]
Co−N1	1.984	1.931	N1−Co−N2	85.1	86.4
Co−N4	1.990	1.979	O1−Co−N2	88.3	88.8
Co−O2	1.899	1.894	O1−Co−O2	178.8	178.5
C8−O2	1.302	1.275	C4−O1−Co	116.8	115.7
C8−O4	1.221	1.238	N1−N2−Co−O1	−92.7	−92.3
C1−C2	1.512	1.448	N1−N2−N3−Co	−4.3	−3.6

[a]Bond lengths are in angstroms, bond angles and dihedral angles in degrees. The corresponding observed value is the mean value of symmetry equivalents. The atom numbering refers to Figure 2.

Relative Ground-State Energies. The relative ground-state energies for the fully optimized structures of 24 Λ-diastereoisomers in aqueous solution are listed in Table 2. To make the comparison more practical, the relative energies with zero-point energy (ZPE) corrections were also calculated and are listed in this table too, as indicated in bold italic font.

Table 2. Relative Energies (in kcal/mol) of the Λ-Diastereoisomers of [Co(EDDA-type)(L)]$^{\pm}$ Chelates with (in Bold Italic Font) or without ZPE Corrections[a]

en-series	[Co(EDDA)(en)]$^+$		[Co(DMEDDA)(en)]$^+$		[Co(DEEDDA)(en)]$^+$	
$\Lambda(SS)(\delta\lambda\delta)(\lambda)$	0.000	***0.000***	0.000	***0.000***	0.000	***0.000***
$\Lambda(SS)(\delta\lambda\delta)(\delta)$	0.414	***0.005***	0.688	***0.785***	0.898	***0.652***
$\Lambda(SS)(\delta\delta\delta)(\lambda)$	4.408	***4.431***	2.025	***1.791***	2.593	***1.885***
$\Lambda(SS)(\delta\delta\delta)(\delta)$	4.591	***4.626***	2.568	***2.800***	3.402	***2.936***
ox-series	[Co(EDDA)(ox)]$^-$		[Co(DMEDDA)(ox)]$^-$		[Co(DEEDDA)(ox)]$^-$	
$\Lambda(SS)(\delta\lambda\delta)$	0.000	***0.000***	0.000	***0.000***	0.000	***0.000***
$\Lambda(SS)(\delta\delta\delta)$	1.862	***1.886***	−0.464	***-0.347***	0.200	***0.131***
edda-series[b]	[Co(EDDA)(CO_3)]$^-$		[Co(EDDA)((S)-ala)]		[Co(EDDA)(mal)]$^-$	
$\Lambda(SS)(\delta\lambda\delta)$	0.000	***0.000***	0.000	***0.000***	0.000	***0.000***
$\Lambda(SS)(\delta\delta\delta)$	1.224	***1.301***	3.086	***3.184***	2.521	***2.688***

[a]All of the stereoisomers are C_2 symmetric except those with bidentate ligands (S)-ala^- and mal^{2-} whose symmetry is C_1. [b]The chelate ring sizes of CO_3^{2-}, (S)-ala^-, and mal^{2-} are 4, 5, and 6, respectively. The chelate ring of (S)-ala^- is δ-twisted.

Before an analysis of the results, it should be emphasized that all of the diastereoisomers in Table 2 have the same Λ-octahedral core and (S)-type chiral nitrogens but differ in the δ/λ twists of the ligands. In which, the twist patterns $(\delta\lambda\delta)$ and $(\delta\delta\delta)$ involve a δ/λ change only in the E-ring of coordinated EDDA-type ligands, because such changes in G-rings cannot yield a stable structure with the $\Lambda(SS)$ configurational chirality.

From Table 2 we see that the ZPE correction significantly affects the energies of the diastereoisomers but does not change their relative stability sequences. For en-series chelates, the relative stability sequences of the $\Lambda(SS)$-diastereoisomers are as follows:

$[Co(EDDA)(en)]^+$:

$$(\delta\lambda\delta)(\lambda) \geq (\delta\lambda\delta)(\delta) > (\delta\delta\delta)(\lambda) > (\delta\delta\delta)(\delta)$$

$[Co(DMEDDA)(en)]^+$:

$$(\delta\lambda\delta)(\lambda) > (\delta\lambda\delta)(\delta) > (\delta\delta\delta)(\lambda) > (\delta\delta\delta)(\delta)$$

$[Co(DEEDDA)(en)]^+$:

$$(\delta\lambda\delta)(\lambda) > (\delta\lambda\delta)(\delta) > (\delta\delta\delta)(\lambda) > (\delta\delta\delta)(\delta)$$

In other words, the relative stability of the $\Lambda(SS)$-diastereoisomers is dominated by the twist of the E-ring of EDDA with the result of $(\delta\boldsymbol{\lambda}\delta) > (\delta\boldsymbol{\delta}\delta)$, while for a given twist pattern of EDDA, it in turn depends on the twist form of en ligand with $(\lambda) > (\delta)$.

For another two series chelates, the relative stability is also the same $(\delta\lambda\delta) > (\delta\delta\delta)$, except for $[Co(DMEDDA)(ox)]^-$ which is $(\delta\lambda\delta) < (\delta\delta\delta)$. Analyses show that this exception is closely related to the planarity of ox^{2-} ligand, which permits the alkyl-substituted (S)-type nitrogens out of the equatorial coordination plane to substantially lower the energy of $(\delta\delta\delta)$ conformer. Similarly, the relative energy of the $(\delta\delta\delta)$ conformer of $[Co(DEEDDA)(ox)]^-$ is also very small, only 0.131 kcal/mol higher than that of the $(\delta\lambda\delta)$ conformer.

In what follows, therefore, we shall focus on the generally most stable $\Lambda(SS)(\delta\lambda\delta)[\delta/\lambda]$ conformers and treat the unique exception separately when it is necessary.

DFT Energy Levels and Kohn−Sham Orbitals. The calculated DFT energy levels and corresponding Kohn−Sham (KS) orbitals of the 24 $\Lambda(SS)$-diastereoisomers are classified according to the irreducible representations (IR) of the molecular point group and compiled in the Supporting Information. As examples, DFT energy levels of the "most" stable $\Lambda(SS)(\delta\lambda\delta)[\lambda/\delta]$ conformers (cf. Table 2) are illustrated in Figure 4. Some selected KS orbitals can be found in Figure S2, parts of them in Figure 5.

Detailed analyses of the KS orbitals revealed that, in all cases, the lowest two unoccupied orbitals are dominated by the d_{xz} and $d_{x^2-y^2}$ atomic orbitals of the central Co(III) ion, forming the typical $\sigma^*_{CoN,CoO}$ antibonding orbitals with the 4 (in the equatorial plane) or 6 (including the axial direction) coordinating atoms, respectively, as depicted in Figure 5. The subsequent unoccupied KS orbitals are mainly $\sigma^*_{CH/NH}$ antibonding orbitals with significant characteristics of Rydberg

dx.doi.org/10.1021/jp403145h | J. Phys. Chem. A 2013, 117, 5061−5072

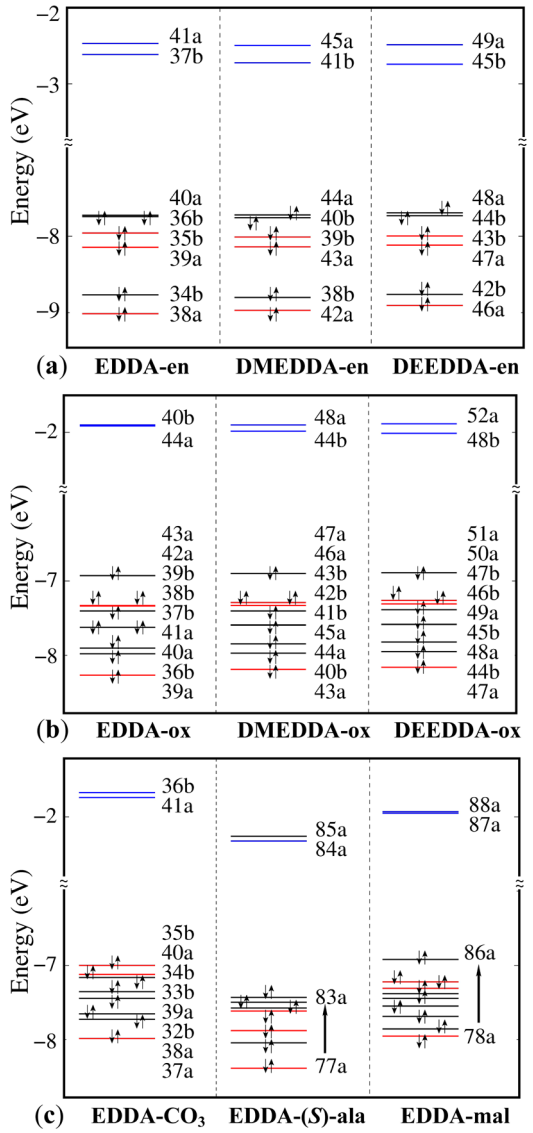

Figure 4. DFT energy levels for the Λ(*SS*)(*δλδ*)[*λ*/*δ*] conformers (cf. Table 2) of the three series of cobalt(III) EDDA type chelates: (a) en-series, (b) ox-series, and (c) edda-series. The levels with red/blue color are dominated by the d-orbitals of the metal ion, as explained in the text.

states.[30] They are separated from the LUMO and LUMO+1 by a big energy gap and thereby not shown in Figure 4. Of the occupied KS orbitals below the HOMO, however, three are dominated by the d_{yz}, d_{xy}, and d_{z^2} orbitals, and their energy levels are indicated by red lines in Figure 4. The splitting pattern of these five d-like KS orbitals is in accordance with the ligand field theory[31,32] (LFT). Correlating the energy levels to other systems with higher symmetries is straightforward as shown in Figure 6a, but correlation of orbitals is complicated by the transformation of coordinate systems (Figure 6b) from O/D_4 to C_2 fields. The corresponding orbital transformation is as follows:

$$d'_{yz} = (d_{yz} + d_{xz})/\sqrt{2} \qquad d'_{xy} = (d_{yz} - d_{xz})/\sqrt{2}$$

$$d'_{xz} = -d_{x^2-y^2} \qquad d'_{z^2} = (\sqrt{3}\,d_{xy} - d_{z^2})/2$$

$$\text{and} \quad d'_{x^2-y^2} = -(\sqrt{3}\,d_{z^2} + d_{xy})/2$$

This makes it possible to identify the orbital features and correlate our DFT results with the early works based on the LFT. The other occupied orbitals are either n_O-type orbitals occupied by the lone pair electrons of carbonyl oxygens, mixed with the σ_{CCO} bonding orbitals of the G-rings, or distorted π_{COO}-type orbitals of the carboxyl groups. They are denoted as $n_O + \sigma_{CCO}$ and π_{COO}, respectively. The latter also have some d−pπ conjugate characteristics due to the participation of some d orbitals.

For instance, the HOMO (e.g., 76th in Figure 5a) and HOMO-1 of the en-series chelates are primarily $n_O + \sigma_{CCO}$ orbitals. Thereby, they are nearly degenerate in energy. The next two occupied orbitals (e.g., 74th and 73rd in Figure 5a) are the $d_{yz} + \pi_{COO}$ and $d_{xy} + \pi_{COO}$ orbitals, respectively. The other occupied lower-energy orbitals are mainly σ/π-type orbitals with or without contributions of d orbitals. Similarly, the HOMO (e.g., 82nd in Figure 5b) of the ox-series complexes is mainly a kidney bean-like n_{ox} orbital distributed on four oxygen atoms of the oxalate ligand, mixed with the σ_{ox} orbital of the ligand. The next two orbitals $d_{xy} + n_O + \sigma_{CCO}$ and $d_{yz} + \pi_{COO} + \pi_{ox}$ are nearly degenerate in energy. The same situation is also found in the $[Co(EDDA)(mal)]^-$ chelate, whose DFT energy levels strongly resemble those of the ox-series complexes due to the similarity of the oxalate and malonate ligands. Interestingly, the highest three occupied orbitals of [Co(EDDA)((*S*)-ala)] are all $n_O + \sigma_{CCO}$ orbitals involving (*S*)-ala, (*S*)-ala+EDDA, and the EDDA backbone, respectively, followed by the d_{yz} and d_{xy} orbitals. In contrast, for the chelate $[Co(EDDA)(CO_3)]^-$, the HOMO and HOMO-1 are $d_{yz} + \pi_{CO3}$ and $d_{xy} + \pi_{CO3} + n_O + \sigma_{CCO}$, followed by three n_O-type orbitals.

To sum up, we found that the HOMO is always an n_O-type orbital for all the compounds except for $[Co(EDDA)(CO_3)]^-$. The KS orbitals dominated by d_{yz} and d_{xy} have some d−pπ conjugate characteristics, while those dominated by $d_{x^2-y^2}$ and d_{xz} exhibit significant coordination bonding and antibonding characteristics. Moreover, beside the 3d orbitals, the 4s and 4p atomic orbitals of the Co(III) ion are also incorporated more or less in the KS orbitals of the chelates, but it is hard to correlate them with the d^2sp^3 hybrid scheme for the central ion. These findings make it possible to clearly interpret the stereochemistry and chiroptical properties of the chelates.

Rotational Strengths and Transition Moments. The calculated excitation energies and oscillator and rotational strengths (both in length and velocity forms) as well as the electric and magnetic transition dipole moments of the 24 Λ-diastereoisomers have been compiled in the Supporting Information. As the rotational strengths calculated in velocity form are independent of the choice of origin, only this form will be addressed below, though no obvious discrepancy between the two forms was observed.

To facilitate discussions, the results for the first six excitations of the lowest energy conformers, which cover the most important spectral range of $\lambda > 350$ nm, are given in Tables 3−5. However, assignments of the excitations are not so easy because they involve many excited configurations or so-called orbital transitions.[33] For example, the major orbital transitions involved in the first excitation $1^1A \rightarrow 2^1A$ of $[Co(EDDA)(en)]^+$ are 73rd→78th (22.7%), 76th→78th (20.1%), 70th→78th (18.7%), and 74th→77th (15.1%). The second excitation $1^1A \rightarrow 1^1B$, they are 74th→78th (37.6%), 68th→78th (19.2%), and 75th→78th (11.0%). To clarify the main features of the excitations, a detailed analysis in terms of chromophore

dx.doi.org/10.1021/jp403145h | J. Phys. Chem. A 2013, 117, 5061−5072

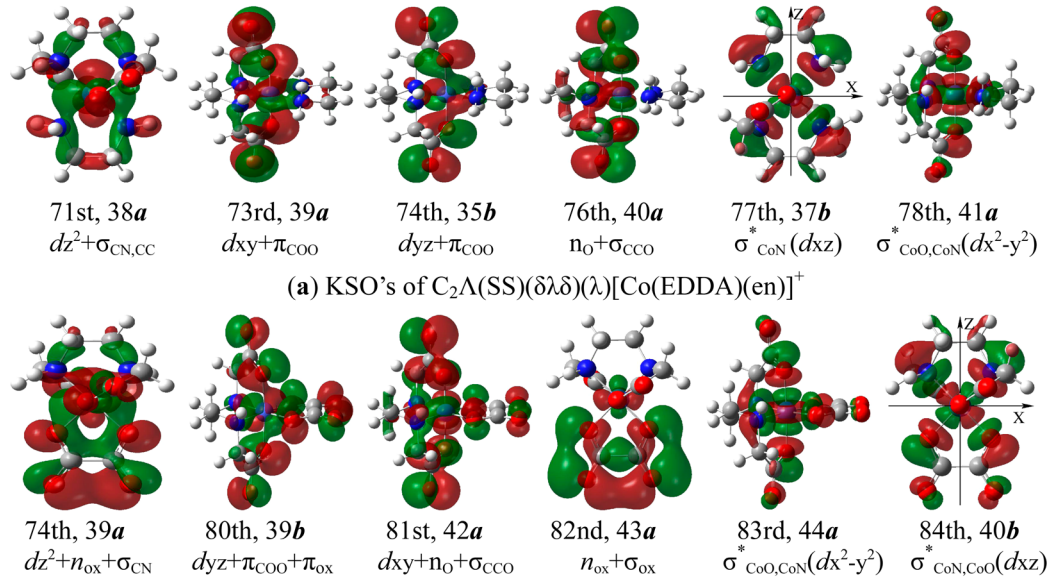

Figure 5. Selected Kohn–Sham orbitals of the chelates (a) $[Co(EDDA)(en)]^+$ and (b) $[Co(EDDA)(ox)]^-$, where ***a*** and ***b*** are the irreducible representations of the orbitals. The related coordinate system is shown in the $\sigma^*(d_{xz})$ orbital.

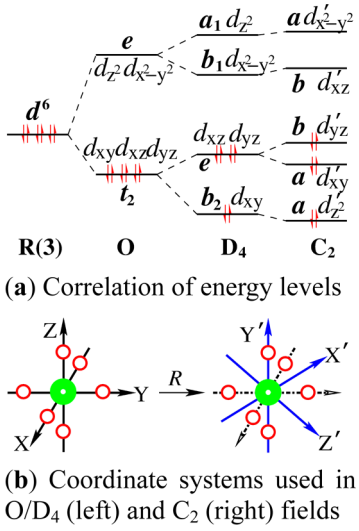

Figure 6. Energy level correlation diagram of d^6 systems and the transformation of coordinate systems from O/D_4 to C_2 fields.

transitions has been carried out carefully, and the dominant contributions are listed in the last column of these tables.

Thus it is clear that all the excitations are characterized by the d–d transitions mixed with some n-σ^* or π–σ^* components. The first three transitions are the typical metal-centered d–d transitions that occur in the long-wavelength range 450–600 nm with large magnetic dipole transition moments of 1.7–1.8 Bohr magneton. The latter three occur in the short-wavelength range 350–410 nm; they are more like the normal ligand-centered n–σ^* or π–σ^* transitions, rather than the n–d or π–d type ligand-to-metal charge transfer (LMCT) transitions, consistent with their small electric and magnetic dipole transition moments. At first glance, such a big difference between the two sets of transitions seems strange, but it is in accord with the magnetic dipole selection rule: $\Delta m = 0, \pm 1$. One simple example is the third transition $d_{z^2} + \sigma_{CN,CC} \rightarrow \sigma^*_{CoN}(d_{xz})$ versus the sixth one $d_{z^2} + \sigma_{CN,CC} \rightarrow \sigma^*_{CoO,CoN}(d_{x^2-y^2})$ in the chelate $[Co(EDDA)(en)]^+$. From the viewpoint of pure d–d transitions, the former ($d_{z^2} \rightarrow d_{xz}$) is magnetic dipole allowed due to $\Delta m = \pm 1$, whereas the latter ($d_{z^2} \rightarrow d_{x^2-y^2}$) is forbidden because of $\Delta m = \pm 2$. Moreover, the former is y-axis polarized, and the corresponding transition moment is $\langle d_{xz}|\mathbf{m}_y|d_{z^2}\rangle = -3^{1/2}i\mu_B$. Its magnitude is very close to the value 1.7496 in Table 3a. This example not only accounts for the big difference between the two classes of transitions but also reveals that the latter three excitations are in fact some magnetic dipole forbidden d–d transitions. Their small electric and negligible magnetic dipole transition moments are partly due to the intrusion of 4p into 3d orbitals, partly borrowed from the ligand-centered n–σ^* or π–σ^* components. For this reason, they will not be discussed in detail later.

As far as the former three excited states are concerned, the first two (2^1A and 1^1B) are derived from the 1^1E level in the D_4 symmetry field[15] and therefore nearly degenerate in energy. The third one (2^1B) is related to the 1^1A_2 level in D_4 symmetry. Thus, we see that the corresponding transitions $1^1A \rightarrow 2^1A$, $1^1A \rightarrow 1^1B$, and $1^1A \rightarrow 2^1B$ will generally produce a major positive CD band and a minor negative one for the chelates.

Calculated and Observed CD Spectra. By use of the excitation energies and rotational strengths calculated at the TDDFT level, theoretical CD spectra of the 24 Λ-diastereoisomers were generated as a sum of Gaussians, centered at the calculated wavelengths λ_{calc} with integral intensities proportional to the rotational strengths R of the corresponding transitions. The half bandwidths Γ at the $\Delta\varepsilon_{max}$/e of Gaussians, were assumed as[34] $\Gamma = k\lambda_{calc}^{3/2}$ with $k = 0.00385$ to best reproduce the experimental spectra. Some of the resulting CD curves, together with the observed[19,21] ones, are displayed in Figure 7. More results can be found in Figures S3–S5.

Clearly, the calculated CD curves for all chelates are in excellent agreement with the observed ones except for some red or blue shifts in the calculated peak wavelengths. Based on this agreement, the characteristics of the experimental CD spectra and related chiral stereochemistry phenomena could be reasonably explained at the first-principle level.

dx.doi.org/10.1021/jp403145h | J. Phys. Chem. A 2013, 117, 5061–5072

Table 3. Symmetries of Excited States (sym), Excitation Wavelengths (λ), Oscillator (f) and Rotational (R) Strengths, and Electric (μ) and Magnetic (m) Dipole Transition Moments as well as the Angle (θ) between Them for the First Six Transitions of the [Co(EDDA-type)(en)]$^+$ Chelates

sym	λ (nm)	f	R(DBM)	$\lvert\mu\rvert$ (D)	$\lvert m\rvert$ (BM)	θ (deg)	assignments[a]
			(a) $C_2\Lambda(SS)(\delta\lambda\delta)(\lambda)$[Co(EDDA)(en)]$^+$				
2^1A	523.38	0.0006	0.4456	0.2651	1.6968	0.0	$d_{xy}(p\pi) + n_O \rightarrow \sigma^*_{CoO,CoN}(d_{x^2-y^2})$
1^1B	523.24	0.0003	−0.2253	0.1728	1.6811	142.2	$d_{yz}(p\pi) + n_O \rightarrow \sigma^*_{CoO,CoN}(d_{x^2-y^2})$
2^1B	462.03	0.0000	−0.0854	0.0548	1.7496	158.3	$d_{z^2} + \sigma_{CN,CC} \rightarrow \sigma^*_{CoN}(d_{xz})$
3^1B	388.18	0.0009	0.0111	0.2777	0.0430	20.5	$d_{xy}(p\pi) + n_O \rightarrow \sigma^*_{CoN}(d_{xz})$
3^1A	387.60	0.0003	−0.0108	0.1586	0.0700	180.0	$d_{yz}(p\pi) + n_O \rightarrow \sigma^*_{CoN}(d_{xz})$
4^1A	330.70	0.0000	0.0005	0.0089	0.0446	0.0	$d_{z^2} + \sigma_{CN,CC} \rightarrow \sigma^*_{CoO,CoN}(d_{x^2-y^2})$
			(b) $C_2\Lambda(SS)(\delta\lambda\delta)(\lambda)$[Co(DMEDDA)(en)]$^+$				
2^1A	533.40	0.0005	0.3880	0.2293	1.7029	0.0	$d_{xy}(p\pi) + n_O \rightarrow \sigma^*_{CoO,CoN}(d_{x^2-y^2})$
1^1B	531.50	0.0004	−0.2968	0.2054	1.6863	151.0	$d_{yz}(p\pi) + n_O \rightarrow \sigma^*_{CoO,CoN}(d_{x^2-y^2})$
2^1B	479.36	0.0000	−0.0007	0.0546	1.7703	91.6	$d_{z^2} + \sigma_{CoN,CN} \rightarrow \sigma^*_{CoN}(d_{xz})$
3^1B	397.16	0.0010	0.0130	0.2840	0.1362	69.3	$d_{xy}(p\pi) + n_O \rightarrow \sigma^*_{CoN}(d_{xz})$
3^1A	395.77	0.0002	−0.0142	0.1347	0.1072	180.0	$d_{yz}(p\pi) + n_O \rightarrow \sigma^*_{CoN}(d_{xz})$
4^1A	333.94	0.0001	−0.0006	0.0724	0.0077	180.0	$d_{z^2} + \sigma_{CoN,CN} \rightarrow \sigma^*_{CoO,CoN}(d_{x-y^2})$
			(c) $C_2\Lambda(SS)(\delta\lambda\delta)(\lambda)$[Co(DEEDDA)(en)]$^+$				
2^1A	538.17	0.0006	0.4290	0.2511	1.7005	0.0	$d_{xy}(p\pi) + n_O \rightarrow \sigma^*_{CoO,CoN}(d_{x^2-y^2})$
1^1B	536.04	0.0005	−0.3608	0.2324	1.6848	160.0	$d_{yz}(p\pi) + n_O \rightarrow \sigma^*_{CoO,CoN}(d_{x^2-y^2})$
2^1B	486.86	0.0000	0.0044	0.0548	1.7761	86.7	$d_{z^2} + \sigma_{CoN,CN} \rightarrow \sigma^*_{CoN}(d_{xz})$
3^1B	401.48	0.0010	0.0242	0.2924	0.1673	60.0	$d_{xy}(p\pi) + n_O \rightarrow \sigma^*_{CoN}(d_{xz})$
3^1A	399.63	0.0002	−0.0177	0.1390	0.1280	180.0	$d_{yz}(p\pi) + n_O \rightarrow \sigma^*_{CoN}(d_{xz})$
4^1A	335.13	0.0001	−0.0008	0.0702	0.0096	180.0	$d_{z^2} + \sigma_{CoN,CN} \rightarrow \sigma^*_{CoO,CoN}(d_{x^2-y^2})$

[a] $d_{xy}(p\pi)$ means $d_{xy} + \pi_{COO}$ with little d−pπ conjugation; n_O is always mixed with the σ_{CCO} orbital of the carboxyl groups.

Table 4. Symmetries of Excited States (sym), Excitation Wavelengths (λ), Oscillator (f) and Rotational (R) Strengths, and Electric (μ) and Magnetic (m) Dipole Transition Moments as well as the Angle (θ) between Them for the First Six Transitions of the [Co(EDDA-type)(ox)]$^+$ Chelates

sym	λ (nm)	f	R(DBM)	$\lvert\mu\rvert$ (D)	$\lvert m\rvert$ (BM)	θ (deg)	assignments[a]
			(a) $C_2\Lambda(SS)(\delta\lambda\delta)(\lambda)$[Co(EDDA)(ox)]$^-$				
1^1B	558.95	0.0010	0.0194	0.3420	1.7408	89.3	$d_{yz}(p\pi) + n_O \rightarrow \sigma^*_{CoO,CoN}(d_{x^2-y^2})$
2^1A	557.31	0.0002	0.2334	0.1408	1.7085	0.0	$d_{xy}(p\pi) + n_O \rightarrow \sigma^*_{CoO,CoN}(d_{x^2-y^2})$
2^1B	496.37	0.0001	−0.1117	0.1145	1.6937	124.6	$d_{z^2} + n_{ox} + \sigma_{CN} \rightarrow \sigma^*_{CoN,CoO}(d_{xz})$
3^1B	394.81	0.0010	0.0053	0.2900	0.0887	79.8	$d_{xy}(p\pi) + n_O \rightarrow \sigma^*_{CoN,CoO}(d_{xz})$
3^1A	394.46	0.0004	−0.0102	0.1797	0.0565	180.0	$d_{yz}(p\pi) + n_O \rightarrow \sigma^*_{CoN,CoO}(d_{xz})$
4^1A	372.09	0.0009	0.0155	0.2682	0.0579	0.0	$d_{z^2} + n_{ox} + \sigma_{CN} \rightarrow \sigma^*_{CoO,CoN}(d_{x^2-y^2})$
			(b) $C_2\Lambda(SS)(\delta\lambda\delta)(\lambda)$[Co(DMEDDA)(ox)]$^-$				
2^1A	567.47	0.0001	0.1784	0.1068	1.7260	0.0	$d_{xy}(p\pi) + n_O \rightarrow \sigma^*_{CoO,CoN}(d_{x^2-y^2})$
1^1B	565.96	0.0009	−0.0642	0.3258	1.7537	97.4	$d_{yz}(p\pi) + n_O \rightarrow \sigma^*_{CoO,CoN}(d_{x^2-y^2})$
2^1B	516.25	0.0001	−0.0306	0.1212	1.6892	98.5	$d_{z^2} + n_{ox} + \sigma_{CN} \rightarrow \sigma^*_{CoN,CoO}(d_{xz})$
3^1B	403.20	0.0010	0.0002	0.2877	0.0066	84.7	$d_{xy}(p\pi) + n_O \rightarrow \sigma^*_{CoN,CoO}(d_{xz})$
3^1A	401.44	0.0001	−0.0082	0.1129	0.0727	180.0	$d_{yz}(p\pi) + n_O \rightarrow \sigma^*_{CoN,CoO}(d_{xz})$
4^1A	378.11	0.0011	0.0051	0.2956	0.0174	0.0	$d_{z^2} + n_{ox} + \sigma_{CN} \rightarrow \sigma^*_{CoO,CoN}(d_{x^2-y^2})$
			(c) $C_2\Lambda(SS)(\delta\lambda\delta)(\lambda)$[Co(DEEDDA)(ox)] $^-$				
2^1A	571.24	0.0001	0.2074	0.1245	1.7243	0.0	$d_{xy}(p\pi) + n_O \rightarrow \sigma^*_{CoO,CoN}(d_{x^2-y^2})$
1^1B	569.25	0.0008	−0.1069	0.3062	1.7512	102.9	$d_{yz}(p\pi) + n_O \rightarrow \sigma^*_{CoO,CoN}(d_{x^2-y^2})$
2^1B	525.04	0.0001	−0.0314	0.1213	1.6981	98.5	$d_{z^2} + n_{ox} + \sigma_{CN} \rightarrow \sigma^*_{CoN,CoO}(d_{xz})$
3^1B	407.29	0.0010	0.0064	0.2930	0.0254	30.5	$d_{xy}(p\pi) + n_O \rightarrow \sigma^*_{CoN,CoO}(d_{xz})$
3^1A	404.98	0.0002	−0.0109	0.1190	0.0912	180.0	$d_{yz}(p\pi) + n_O \rightarrow \sigma^*_{CoN,CoO}(d_{xz})$
4^1A	379.30	0.0010	0.0049	0.2875	0.0172	0.0	$d_{z^2} + n_{ox} + \sigma_{CN} \rightarrow \sigma^*_{CoO,CoN}(d_{x^2-y^2})$

[a] Here, $d_{xy}(p\pi)$ means $d_{xy} + \pi_{COO} + \pi_{ox}$ with little d−pπ conjugation; n_{ox} is always mixed with the σ_{ox} orbital of the oxalate ligand. See footnotes of Table 3 for other information.

Generally speaking, the observed CD curves each consists of three absorption bands: a major positive band around 550 nm arising from the first two d−d transitions that are nearly degenerate in energy (cf. Tables 3−5); a minor negative or nearly vanishing band around 480 nm originating from the third d−d transition, and a weak positive or negligible band around 380 nm which can be ascribed to the latter three ligand-centered $n-\sigma^*/\pi-\sigma^*$ transitions, as mentioned before.

For unsubstituted EDDA chelates, the first CD band or Cotton effect is positive, and the second one is negative. This typical CD pattern is consistent with the Λ-octahedral core of the chelates defined by the pseudo-C_3 axis (Figure 2) and also

dx.doi.org/10.1021/jp403145h | J. Phys. Chem. A 2013, 117, 5061−5072

Table 5. Symmetries of Excited States (sym), Excitation Wavelengths (λ), Oscillator (f) and Rotational (R) Strengths, and Electric (μ) and Magnetic (m) Dipole Transition Moments as well as the Angle (θ) between Them for the First Six Transitions of the $[Co(EDDA)(L)]^n$ (L = CO_3^{2-}, (*S*)-ala$^-$, mal^{2-}) Chelates

sym	λ (nm)	f	R(DBM)	$\|\mu\|$ (D)	|m| (BM)	θ (deg)	assignments[a]
				(a) $C_2\Lambda(SS)(\delta\lambda\delta)(\lambda)[Co(EDDA)(CO_3)]^-$			
2^1A	582.24	0.0001	0.1773	0.1101	1.7297	0.0	$d_{xy}(p\pi)_{CO3} + n_O \rightarrow \sigma^*_{CoO,CoN}(d_{x^2-y^2})$
1^1B	580.89	0.0011	0.0476	0.3622	1.7202	86.4	$d_{yz}(p\pi)_{CO3} + n_O \rightarrow \sigma^*_{CoO,CoN}(d_{x^2-y^2})$
2^1B	479.08	0.0002	−0.0865	0.1583	1.8489	107.5	$d_{z^2} + n_{CO3} + \pi_{COO} \rightarrow \sigma^*_{CoN,CoO}(d_{xz})$
3^1B	400.79	0.0010	0.0090	0.2929	0.0703	64.4	$d_{xy}(p\pi)_{CO3} + n_O \rightarrow \sigma^*_{CoN,CoO}(d_{xz})$
3^1A	396.14	0.0003	−0.0029	0.1614	0.0179	180.0	$d_{yz}(p\pi)_{CO3} + n_O \rightarrow \sigma^*_{CoN,CoO}(d_{xz})$
4^1A	370.11	0.0006	0.0063	0.2224	0.0285	0.0	$d_{z^2} + n_{CO3} + \pi_{COO} \rightarrow \sigma^*_{CoO,CoN}(d_{x^2-y^2})$
				(b) $C_1\Lambda(SS)(\delta\lambda\delta)(\delta)$[Co(EDDA)((*S*)-ala)]			
2^1A	560.88	0.0005	0.1024	0.2521	1.7133	76.3	$d_{yz} + n_O + n_{ala} \rightarrow \sigma^*_{CoO,CoN}(d_{x^2-y^2})$
3^1A	516.62	0.0003	0.0895	0.1929	1.7103	74.0	$d_{xy}(p\pi) + n_O \rightarrow \sigma^*_{CoO,CoN}(d_{x-y^2})$
4^1A	476.14	0.0001	−0.0811	0.0872	1.7273	123.7	$d_{z^2} + \sigma_{ala} \rightarrow \sigma^*_{CoN,CoO}(d_{xz})$
5^1A	397.62	0.0008	−0.0161	0.2579	0.0954	130.9	$d_{yz} + n_O + n_{ala} \rightarrow \sigma^*_{CoN,CoO}(d_{xz})$
6^1A	378.94	0.0006	0.0027	0.2253	0.0679	81.1	$d_{xy}(p\pi) + n_O \rightarrow \sigma^*_{CoN,CoO}(d_{xz})$
7^1A	350.88	0.0003	0.0018	0.1551	0.0238	59.9	$d_{z^2} + \sigma_{ala} \rightarrow \sigma^*_{CoO,CoN}(d_{x^2-y^2})$
				(c) $C_1\Lambda(SS)(\delta\lambda\delta)(\lambda)[Co(EDDA)(mal)]^-$			
2^1A	567.30	0.0011	0.0292	0.3585	1.7486	88.6	$d_{yz}(p\pi)_{mal} + n_O \rightarrow \sigma^*_{CoO,CoN}(d_{x^2-y^2})$
3^1A	563.31	0.0002	0.2197	0.1489	1.7183	27.4	$d_{xy}(p\pi)_{mal} + n_O \rightarrow \sigma^*_{CoO,CoN}(d_{x^2-y^2})$
4^1A	507.36	0.0001	−0.1448	0.0942	1.7664	148.1	$d_{z^2} + \pi_{mal} + \pi_{COO} \rightarrow \sigma^*_{CoN,CoO}(d_{xz})$
5^1A	398.66	0.0004	−0.0074	0.1790	0.1487	106.5	$d_{yz}(p\pi)_{mal} + n_O \rightarrow \sigma^*_{CoN,CoO}(d_{xz})$
6^1A	396.36	0.0011	0.0017	0.3107	0.1100	88.4	$d_{xy}(p\pi)_{mal} + n_O \rightarrow \sigma^*_{CoN,CoO}(d_{xz})$
7^1A	372.59	0.0001	0.0064	0.0893	0.0976	40.7	$d_{z^2} + \pi_{mal} + \pi_{COO} \rightarrow \sigma^*_{CoO,CoN}(d_{x^2-y^2})$

[a] $d_{xy}(p\pi)_{mal}$ and $d_{xy}(p\pi)_{CO3}$ mean $d_{xy} + \pi_{mal}$ and $d_{xy} + \pi_{CO3}$, respectively, both exhibit some d-pπ conjugate characteristics. See footnotes of Table 3 for other information.

in conformity with the left-handed helix (λ) of the EDDA ligand designated using the C_2 axis.

For substituted EDDA chelates, only the first positive CD band is remarkable, but its intensity is less than one-half of the unsubstituted counterparts. This reduction in intensities of the first CD bands was ascribed to the difference in vicinal effects induced by the asymmetric nitrogen donor atoms of related complexes. Moreover, the vanishing of the second CD band leads to another issue, which will be discussed later.

It should be pointed out that, in the comparison of calculated and observed CDs (Figure 7), only the generally most stable $\Lambda(SS)(\delta\lambda\delta)[\delta/\lambda]$ conformers have been taken into consideration. This may not be adequate for the chelates $[Co(EDDA)(en)]^+$, $[Co(DMEDDA)(ox)]^-$, and $[Co(DEEDDA)(ox)]^-$, because their less stable conformers are energetically very closer to the most stable ones (Table 2). For this reason, their Boltzmann-weighted CD curves at room temperature have been calculated as shown in Figure 8. Though no visible changes in band shapes are found, these averaged CDs are significantly better than the lowest energy conformers', as far as the wavelengths of the major CD bands are concerned. In addition, a weak positive peak around 383 nm appears in the averaged CD of $[Co(EDDA)(en)]^+$, which is also in line with the observed CD.

So far our discussions have been concentrated on the CD curves of the lowest energy conformers. By inspection of all the CD curves (Figures S3−S5), we see that the twist form (δ/λ) of the E-ring in the EDDA backbone dominates the long-wavelength range of λ>500 nm by altering the order of the first two transitions. For chelates with λ-twisted E-ring, there is one positive major CD band around 550 nm, while for those with δ-twisted E-ring, there are two CD bands in the range with the first being negative, and the second, positive. In other words, the twist form (δ/λ) of the E-ring is also an important factor beside the (Δ/Λ) octahedral core in determining the sign of CD bands for these chelates.

Chelate-Ring Size Effects of Rotational Strengths. In the edda-series complexes, the bidentate ligands CO_3^{2-}, (*S*)-ala$^-$ (including ox^{2-} and en) and mal^{2-}, chelate with the central metal ion forming four-, five-, and six-membered chelate rings, respectively. Many studies in the literature have concentrated on the effects of chelate ring size on the CD intensities or rotational strengths of the edda-series chelates.

For the *s-cis*-isomers, Van Saun and Douglas[19] found that rotational strengths of the d−d transitions are determined largely by the EDDA backbone and quite insensitive to the bidentate ligand used. According to our calculations, this conclusion can be confirmed, because the calculated total rotational strengths of the major CD bands of the edda-series chelates are: CO_3^{2-} 0.2249; ox^{2-} 0.2528, (*S*)-ala$^-$ 0.1919, en 0.2203; mal^{2-} 0.2489. They do not exhibit any tendency on the ring size (even only the dianion series CO_3^{2-}, ox^{2-}, and mal^{2-}, are considered) but fluctuate from 0.19 to 0.25 with a mean value of 0.23 DBM.

Later on, Jordan and Legg[20] studied the *uns-cis*-isomers of the dianion series and pointed out that the net rotational strengths as well as the dominant peak intensities, decrease in the order CO_3^{2-} > ox^{2-} > mal^{2-}, with increasing the chelate ring size. Normally one thought that if this were correct, the same trend would also be observed in the *s-cis*-isomers, but it was not observed as we have stated. There must be something different between the two series isomers, therefore.

To solve this issue, calculations for the *uns-cis*-isomers of the dianion series chelates have been done using the same functional and basis set. The results show that the most stable conformers have the chiral form $C_1\Lambda(RS)(\lambda\delta\lambda)$, and the less stable conformers are mainly in the form $C_1\Lambda(RR)(\lambda\lambda\delta)$. Like the *s-cis*-isomers, the first three excitations in the *uns-cis*-isomers

dx.doi.org/10.1021/jp403145h | J. Phys. Chem. A 2013, 117, 5061−5072

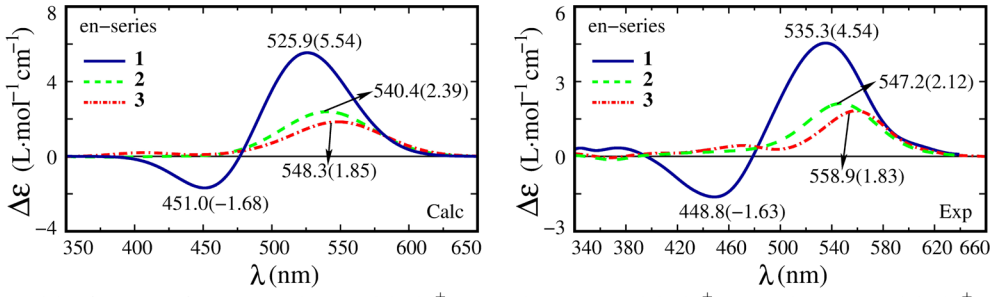

(**a**) The en-series : **1** [Co(EDDA)(en)]$^+$, **2** [Co(DMEDDA)(en)]$^+$, **3** [Co(DEEDDA)(en)]$^+$

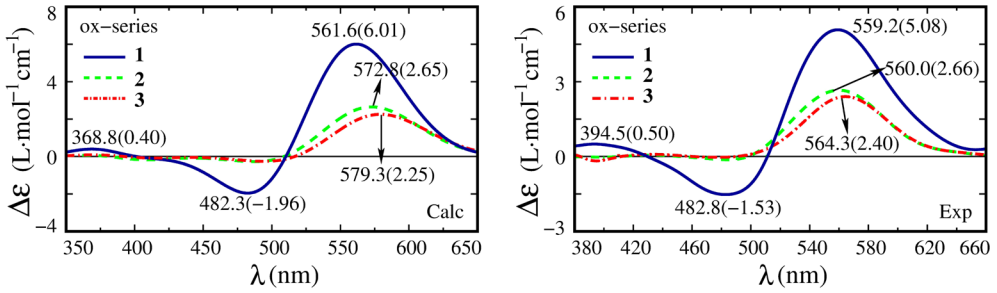

(**b**) The ox-series: **1** [Co(EDDA)(ox)]$^-$, **2** [Co(DMEDDA)(ox)]$^-$, **3** [Co(DEEDDA)(ox)]$^-$

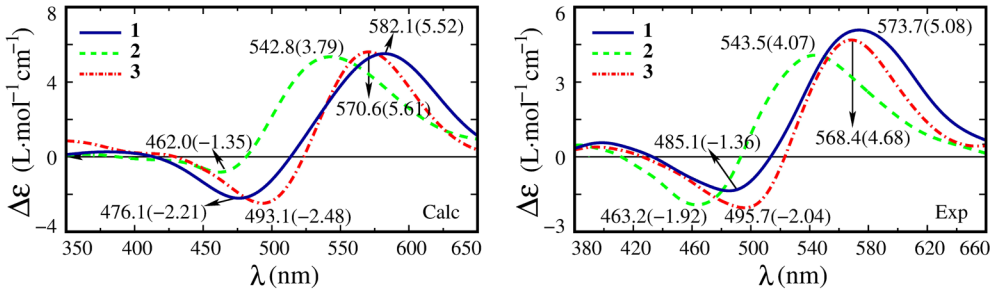

(**c**) The edda-series: **1** [Co(EDDA)(CO_3)]$^-$, **2** [Co(EDDA)((*S*)-ala)], **3** [Co(EDDA)(mal)]$^-$

Figure 7. Comparison of the calculated (left) and observed[19,21] (right) CD spectra of the conformers: (a) the en-series $C_2\Lambda(SS)(\delta\lambda\delta)(\lambda)$, (b) the ox-series $C_2\Lambda(SS)(\delta\lambda\delta)$, and (c) the edda-series (**1**) $C_2\Lambda(SS)(\delta\lambda\delta)$, (**2**) $C_1\Lambda(SS)(\delta\lambda\delta)(\delta)$, and (**3**) $C_1\Lambda(SS)(\delta\lambda\delta)$. Numbers beside the CD curves are the λ_{max} and $\Delta\varepsilon_{max}$ (in parentheses) of the related CD bands, respectively.

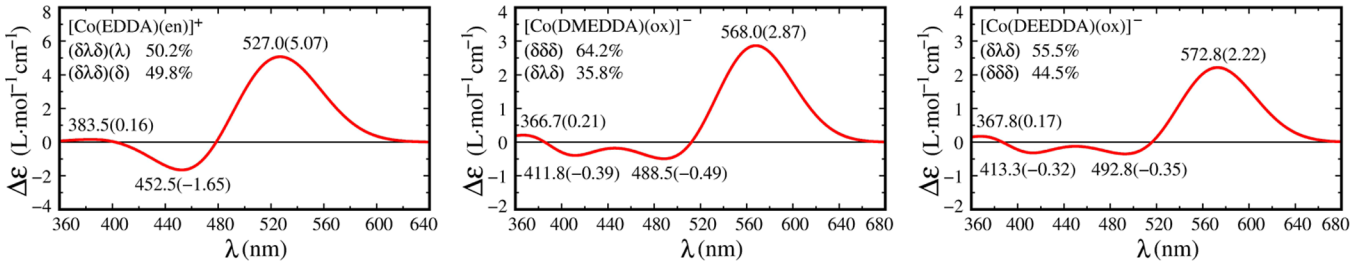

Figure 8. Boltzmann-weighted CD spectra for the two lowest energy conformers of the chelates [Co(EDDA)(en)]$^+$, Co(DMEDDA)(ox)]$^-$, and [Co(DEEDDA)(ox)]$^-$.

originate from the typical d−d transitions mixed with some n−σ^* or $\pi-\sigma^*$ components. But neither the first two nor the last two excitations are nearly degenerate in energy, which means that they cannot be viewed as a perturbation of levels in O/D_4 symmetry field. In this point, the *uns-cis*-isomers are quite different from the *s-cis*-isomers. The calculated CD curves for the most stable *uns-cis*-$C_1\Lambda(RS)(\lambda\delta\lambda)$ conformers, together with the observed ones, are displayed in Figure 9. What we found for the ring-size effects is that the net rotational strengths or integral intensities of the dominant CD bands indeed follow the order CO_3^{2-} > ox^{2-} > mal^{2-}, but the peak intensities do not. Astonishingly, if the contributions of less stable *uns-cis*-$C_1\Lambda(RR)(\lambda\lambda\delta)$ conformers are taken into consideration, the Boltzmann-weighted CD curves for chelates **1** and **2** are nearly identical with the observed ones (the dominant peak intensities increase to 2.75 and 1.94, and the corresponding wavelengths shift to 551.7 and 550.0 nm, respectively), while for chelate **3** only the weak positive CD band around 389 nm becomes negative, as expected. In this sense, we could say that Jordan and Legg's conclusion has been theoretically confirmed.

dx.doi.org/10.1021/jp403145h | J. Phys. Chem. A 2013, 117, 5061−5072

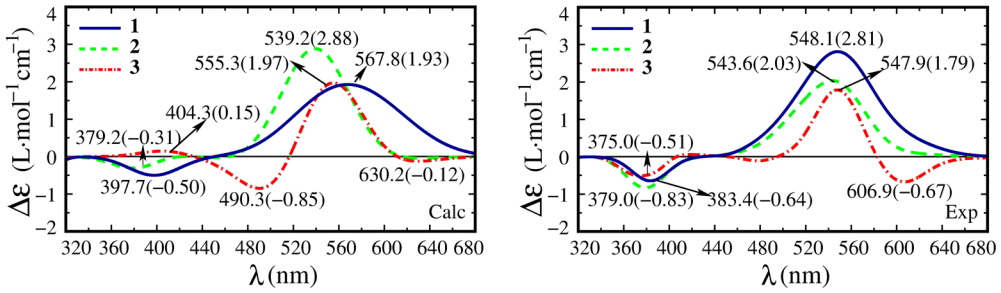

Figure 9. Calculated (left) and observed[20] (right) CD spectra of the *uns-cis*-Λ(*RS*)(*λδλ*) conformers of the chelates: (**1**) Co(EDDA)$(CO_3)]^-$, (**2**) [Co(EDDA)(ox)]$^-$, and (**3**) [Co(EDDA)(mal)]$^-$.

Table 6. Calculated *N*-Vicinal Effects in the Chelates C_2Λ(*SS*)(*δλδ*)(*λ*)[Co(EDDA)(en)]$^+$ and C_2Λ(*SS*)(*δλδ*)(*λ*)[Co(EDDA)(ox)]$^-$

		CD-band intensities (DBM)			*N*-vicinal effects (DBM)				
chelate	CD-band[a]	optim[b]	fixed[c]	EDDA	total	substitution		relaxation	
en	1	0.0682	0.0916	0.2203	0.1521	0.1287	85%	0.0234	15%
	2	0.0044	−0.0230	−0.0854	−0.0898	−0.0625	70%	−0.0273	30%
ox	1	0.1004	0.1247	0.2528	0.1523	0.1281	84%	0.0243	16%
	2	−0.0314	−0.0467	−0.1117	−0.0804	−0.0650	81%	−0.0154	19%

[a]The first CD band involves two transitions $1^1A \rightarrow 2^1A$, $1^1A \rightarrow 1^1B$; the second one is $1^1A \rightarrow 2^1B$. [b]Rotational strengths for the optimized geometries of corresponding DEEDDA chelates. [c]Rotational strengths for the geometries of DEEDDA chelates constructed from those of EDDA chelates by replacing the hydrogen atoms on the asymmetric nitrogens with the ethyl groups without geometry reoptimization.

However, since the calculated curve shape for chelate **3** is still significantly different from the observed one at about 490 nm and 610 nm, more theoretical work is needed before this discrepancy can be explained.

What we learn from the above discussions is that the influence of chelate-ring size of the bidentate ligands depends on the symmetry of the cobalt-EDDA backbone. This could be easily understood according to the perturbation theory. For the *s-cis*-isomers, the cobalt-EDDA backbone is C_2-symmetric, and the dianion bidentate ligands are also C_2-symmetric (carbonate, oxalate) or pseudo-C_2-symmetric (malonate). Thus, the perturbation of the ring size (one possible measure for this is the bite angle O−Co−O) of bidentate ligands to the energy levels or CD intensities of the chelates is "symmetric". However, for the *uns-cis*-isomers, the cobalt-EDDA backbone is unsymmetric (C_1), and the corresponding perturbation is also "un-symmetric". It is known that a symmetric perturbation usually shifts the energy levels of *d*-orbitals as a whole, while the unsymmetric perturbation can significantly change the energy levels as well as the integral CD intensities of the chelates. Since a smaller bite angle means a larger perturbation, this accounts for, at least qualitatively, why the ring-size effects (CO_3^{2-} > ox^{2-} > mal^{2-}) were only observed in the *uns-cis*-isomers.

Vicinal Effects of Asymmetric Nitrogens. For the en- and ox-series chelates, the vicinal effects due to the asymmetric nitrogens of the coordinated EDDA were experimentally measured[21] by subtracting the CD curves of the DEEDDA complexes from those of the corresponding EDDA ones. The use of the DEEDDA complexes as the reference compounds is because the asymmetric nitrogens in these complexes make negligible contribution to their optical activity due to all the groups about the nitrogen being similar, differing only in the third atom from the nitrogen. Theoretically, it is convenient to calculate the vicinal effects as differences in rotational strengths of corresponding CD absorption bands instead of the CD curves. As examples, the vicinal effects for the lowest energy conformers of the chelates [Co(EDDA)(en)]$^+$ and [Co(EDDA)(ox)]$^-$ have been calculated by subtracting the rotational strengths of the optimized DEEDDA chelates (third column of Table 6) from those of the corresponding EDDA ones (fifth column), and the results are listed in the sixth column of Table 6. These values are referred to as the total vicinal effects and can be directly compared with the experimental values. Besides, since the optimized geometries of related DEEDDA complexes are different from those of EDDA chelates, the total vicinal effects incorporate both the substitutent effects and conformational relaxation effects resulting from replacing EDDA with DEEDDA. The substitutent effects, which might be the purely vicinal effects, have therefore been calculated by first replacing the hydrogen atoms on the asymmetrical nitrogens of EDDA complexes with the ethyl groups without geometry reoptimization, then subtracting their rotational strengths (fourth column) from the corresponding EDDA compounds (fifth column). The results are given in the seventh column of Table 6. As seen from this table, the substitutent effects are the dominant components of the *N*-vicinal effects. The conformational relaxation effects, as differences between the total vicinal and the substitutent effects, are minor but cannot be neglected. Interestingly, both effects are positive for the first CD band and negative for the second ones. Thus, they make synergistic contributions to the *N*-vicinal effects as well as the chiroptical properties of the chelates.

Contribution of Chiral Arrays to the CD Spectra. The chiroptical properties of a molecule are theoretically determined by the rotational strengths of related transitions in the molecule. For metal complexes, the rotational strengths of d−d transitions are principally governed by the Δ/Λ distribution of chelate rings about the central metal ion, the *δ*/*λ* conformations of the chelate rings, and the vicinal effects of *R*/*S* asymmetric donor atoms of the ligands. The contributions from these three are thought to be additive, as demonstrated by the

dx.doi.org/10.1021/jp403145h | J. Phys. Chem. A 2013, 117, 5061−5072

Table 7. Mean Contributions of the Chiral Arrays to the Rotational Strengths of ox-Series Chelates[a]

	[Co(EDDA)(ox)]$^-$		[Co(DMEDDA)(ox)]$^-$		[Co(DEEDDA)(ox)]$^-$		[Co(EDDA)(CO_3)]$^-$	
sym	Λ_{SS}	δ_E	Λ_{SS}	δ_E	Λ_{SS}	δ_E	Λ_{SS}	δ_E
2^1A	0.2649	0.0315	0.2432	0.0648	0.2718	0.0644	0.2092	0.0160
1^1B	−0.0321	−0.0515	−0.1202	−0.0560	−0.1696	−0.0627	0.0147	−0.0329
sum[b]	0.2328	−0.0200	0.1230	0.0088	0.1022	0.0017	0.2239	−0.0169
2^1B	−0.1103	0.0014	−0.0436	−0.0130	−0.0417	−0.0103	−0.0898	0.0033

[a]Including the carbonate chelate due to the similarity. [b]The sum of contributions to the first two transitions or to the first CD band.

Table 8. Mean Contributions of the Chiral Arrays to the Rotational Strengths of en-Series Chelates

	[Co(EDDA)(en)]$^+$			[Co(DMEDDA)(en)]$^+$			[Co(DEEDDA)(en)]$^+$		
sym	Λ_{SS}	δ_E	δ_{en}	Λ_{SS}	δ_E	δ_{en}	Λ_{SS}	δ_E	δ_{en}
2^1A	0.5097	0.0708	−0.0101	0.4842	0.0962	−0.0076	0.5239	0.0868	−0.0050
1^1B	−0.3182	−0.0830	−0.0083	−0.4004	−0.0891	−0.0070	−0.4728	−0.0890	−0.0125
sum[a]	0.1915	−0.0122	−0.0184	0.0838	0.0071	−0.0146	0.0511	−0.0022	−0.0175
2^1B	−0.0767	0.0082	0.0024	−0.0087	−0.0088	0.0024	−0.0040	−0.0085	0.0019

[a]The sum of contributions to the first two transitions or to the first CD band.

experimental evidence[35] and theoretical works.[25,36] If we assume that the rotational strength of a given transition can be expressed as a sum of contributions, each associated with one chiral array in the chelate, such contributions can then be determined by the rotational strengths of a given transition in different diastereoisomers with the same molecular symmetry.

For the ox-series chelates, the related diastereoisomers $C_2\Lambda(SS)(\delta\boldsymbol{\lambda}\delta)$ and $C_2\Lambda(SS)(\delta\boldsymbol{\delta}\delta)$ are different only in the twist form (δ/λ) of the E-ring. Thus, two phenomenological parameters, δ_E and Λ_{SS}, are needed to represent the contributions of δ-twisted E-ring and the remaining part $\Lambda(SS)(\delta\ \delta)$, respectively, because the contribution of λ-twisted E-ring must be $-\delta_E$. They can be expressed as: $\Lambda_{SS} = (\boldsymbol{b} + \boldsymbol{a})/2$, $\delta_E = (\boldsymbol{b} - \boldsymbol{a})/2$; where $\boldsymbol{a}$ and $\boldsymbol{b}$ are the rotational strengths of a given transition in the diastereoisomers $C_2\Lambda(SS)(\delta\boldsymbol{\lambda}\delta)$ and $C_2\Lambda(SS)(\delta\boldsymbol{\delta}\delta)$, respectively. The results for the first three transitions are tabulated in Table 7.

Similarly, for the en-series chelates, an additional parameter δ_{en} is needed to represent the contribution of δ-twisted en ligand. The related expressions are as follows: $\Lambda_{SS} = (\boldsymbol{d} + \boldsymbol{c} + \boldsymbol{b} + \boldsymbol{a})/4$, $\delta_E = (\boldsymbol{d} + \boldsymbol{c} - \boldsymbol{b} - \boldsymbol{a})/4$, and $\delta_{en} = (\boldsymbol{d} - \boldsymbol{c} + \boldsymbol{b} - \boldsymbol{a})/4$; where $\boldsymbol{a}$, $\boldsymbol{b}$, $\boldsymbol{c}$, and $\boldsymbol{d}$ are the rotational strengths of a given transition in the diastereoisomers $C_2\Lambda(SS)(\delta\lambda\delta)(\lambda)$, $C_2\Lambda(SS)(\delta\lambda\delta)(\delta)$, $C_2\Lambda(SS)(\delta\delta\delta)(\lambda)$, and $C_2\Lambda(SS)(\delta\delta\delta)(\delta)$, respectively. The results for the first three transitions are listed in Table 8.

As expected, in the two series chelates, the parameter Λ_{SS}, which is the sum of contributions from the Λ-octahedral core, the *S*-type chiral nitrogens, and the δ-twisted G-rings, is the dominating factor for all the three transitions, especially for the first two, while the contribution of E-ring (δ_E) is much less than the Λ_{SS} in magnitude. In the en series, the influence of the en ligand (δ_{en}) on the sum of first two transitions (third row in Table 8) is comparable to the δ_E, though it is negligible for each of the transitions. Moreover, for the first transitions $1^1A \rightarrow 2^1A$ of ox/en series, the Λ_{SS} does not change very much from EDDA (0.2649/0.5097) to DEEDDA (0.2718/0.5239) chelates, while for the second transitions $1^1A \rightarrow 1^1B$, it rapidly increases in magnitude but is opposite in sign. This leads to the sum of contributions to the first two transitions, or to the first CD bands, sharply declining from EDDA (0.2328/0.1915) to DMEDDA (0.1230/0.0838) or to DEEDDA (0.1022/0.0511) chelates. Clearly, such a sharp decline in Λ_{SS} is directly related to the vicinal effects of the *S*-type chiral nitrogens. Thus, the parameter Λ_{SS} could serve as a good measure for the vicinal effects of the chiral nitrogens.

To get a deep insight into the parameter Λ_{SS}, correlations to the net charges of chiral nitrogens have been made, but insufficient evidence is available in support of this argument. Nevertheless, we found that the twist angles (Table 9) of E-ring in these chelates have a good inverse correlation to the values of Λ_{SS}, and therefore, to the vicinal effects. In both en- and ox-series, from EDDA to DMEDDA the twist angle of E-ring increases about 4°, while from DMEDDA to DEEDDA, it is nearly unchanged. In other words, the twist angle of E-ring is the key structural factor controlling the vicinal effects of asymmetric nitrogens in these chelates.

Table 9. Optimized Twist Angles of E-Ring and G-Rings in the [Co(EDDA-type)(L)]$^\pm$ Chelates[a]

en-series	[Co(EDDA)(en)]$^+$		[Co(DMEDDA)(en)]$^+$		[Co(DEEDDA)(en)]$^+$	
$\Lambda(SS)(\delta\lambda\delta)(\lambda)$	50.65	***14.17***	54.08	***13.00***	54.60	***12.55***
$\Lambda(SS)(\delta\lambda\delta)(\delta)$	50.93	***14.72***	54.23	***14.56***	55.08	***13.12***
$\Lambda(SS)(\delta\delta\delta)(\lambda)$	49.61	***18.72***	54.36	***19.65***	55.40	***19.57***
$\Lambda(SS)(\delta\delta\delta)(\delta)$	49.58	***20.18***	54.82	***21.33***	55.92	***21.11***
ox-series	[Co(EDDA)(ox)]$^-$		[Co(DMEDDA)(ox)]$^-$		[Co(DEEDDA)(ox)]$^-$	
$\Lambda(SS)(\delta\lambda\delta)$	48.40	***14.00***	51.70	***13.51***	52.36	***12.94***
$\Lambda(SS)(\delta\delta\delta)$	48.27	***19.25***	52.71	***20.27***	52.96	***19.78***
edda-series[b]	[Co(EDDA)(CO_3)]$^-$		[Co(EDDA)((*S*)-ala)]		[Co(EDDA)(mal)]$^-$	
$\Lambda(SS)(\delta\lambda\delta)[\delta]$	48.44	***14.38***	49.68	***14.26***	48.44	***14.42***
$\Lambda(SS)(\delta\delta\delta)[\delta]$	48.51	***19.66***	48.29	***19.01***	47.72	***19.28***

[a]Angles are in degrees. The roman type is for E-ring, bold italics for G-rings. [b]The chelate ring sizes of CO_3^{2-}, (*S*)-ala$^-$, and mal^{2-} are 4, 5, and 6, respectively. The chelate ring of (*S*)-ala$^-$ is δ-twisted.

CONCLUSIONS

In this paper, we have presented a detailed theoretical analysis on the chiroptical properties of a series of cobalt(III) complexes with EDDA-type ligands at the DFT/B3LYP/6-311++G(2d,p) level of theory, with special efforts made in understanding the

dx.doi.org/10.1021/jp403145h | J. Phys. Chem. A 2013, 117, 5061−5072

chelate ring-size effects as well as the vicinal effects of asymmetric nitrogens. The 24 possible *s-cis-* and 6 *uns-cis-*Λ-diastereoisomers of the complexes have been optimized and used in this work. The calculated CD curves for all the chelates are in excellent agreement with the observed ones except for some small red or blue shifts in the calculated peak wavelengths. Based on this agreement, the characteristics of the experimental CD spectra and related chiral stereochemistry phenomena have been discussed. The main conclusions are as follows:

(1) The influence of chelate-ring size of the bidentate ligands on the CD intensities depends on the symmetry of the cobalt-EDDA backbone. This can be well understood according to the perturbation theory. For the *s-cis*-isomers, the influence is negligible due to the perturbation is symmetric. For the *uns-cis*-isomers, the perturbation is unsymmetric. Since a small ring size means a large perturbation, this makes the integral CD intensities decrease with increasing the chelate ring size.

(2) The vicinal effects of asymmetric nitrogrns involve both the substitutent and conformational changes. Both changes make synergistic contributions to the *N*-vicinal effects, with the former being dominant.

(3) The twist form (δ/λ) of the backbone ethylenediamine (E) ring of the coordinated EDDA-type ligands is a key factor to understand the chiroptical properties of these chelates: It not only dominates the relative stabilities of the *s-cis*-Λ(*SS*)-diastereoisomers with the result that $\lambda > \delta$ but also affects the major CD band by changing the order of the first two transitions. Moreover, the twist angle of the E-ring is inversely related to the vicinal effect of chiral nitrogens.

These findings may help us to understand the chelate-ring size as well as vicinal effect related chiroptical phenomenon of the cobalt EDDA-type chelates.

■ ASSOCIATED CONTENT

Supporting Information

Optimized geometries (Figure S1), Kohn−Sham orbitals (Figure S2), excitation energies, oscillator and rotational strengths, the calculated ECD spectra (Figures S3−S5) for different diastereoisomers of the cobalt(III) EDDA-type complexes, as well as full citations for refs 27 and 33. This material is available free of charge via the Internet at http://pubs.acs.org.

■ AUTHOR INFORMATION

Corresponding Author

*E-mail: ykwang@sxu.edu.cn.

Notes

The authors declare no competing financial interest.

■ ACKNOWLEDGMENTS

We gratefully acknowledge funding from the National Natural Science Foundation of China (Grant No. 21273139).

■ REFERENCES

(1) Mori, M.; Shibata, M.; Kyuno, E.; Maruyama, F. The Cobalt (III) Complexes of Ethylenediaminediacetic and Ammoniadiacetic Acids. *Bull. Chem. Soc. Jpn.* **1962**, *35*, 75−77.

(2) Sabo, T. J.; Grguric-Sipka, S. R.; Trifunovic, S. R. Transition Metal Complexes with EDDA-Type Ligands—a Review. *Synth. React. Inorg. Met. Org. Chem.* **2002**, *32*, 1661−1717.

(3) Yano, S.; Murata, T.; Asami, M.; Inoue, M.; Yashiro, M.; Kosaka, M.; Yoshikawa, S. A Novel Isomer of *s-cis*-[Co(edda-type)(*L*)] (edda = Ethylenediamine-*N*,*N*′-diacetate; *L* = One Bidentate or Two Unidentate Ligands) Containing Equatorially Oriented N-CH_2 Bonds of the Acetate Arms. Crystal Structure of *s-cis*-[*N*,*N*′-Dimethyl-(1*R*,2*R*)-1,2-cyclohexanediamine-*N*,*N*′-diacetato] (ethylenediamine) cobalt(III) Perchlorate, *s-cis*-[Co(*N*,*N*′-Me_2-*R*,*R*-chxnda)(en)]ClO_4. *Inorg. Chem.* **1984**, *23*, 4127−4128.

(4) Das, K.; Sinha, U. C.; Phulambrikar, A.; Chatterjee, C.; Bohra, R. Structure of (Ethylenediamine)(*cis*-α-ethylenediamine-*N*,*N*′-diacetato) Cobalt(III) Perchlorate. *Acta Crystallogr.* **1989**, *C45*, 398−400.

(5) Brubaker, G. R.; Schaefer, D. P.; Worrell, J. H.; Legg, J. I. Complexes of Cobalt(III) with Flexible Tetradentate Ligands. *Coord. Chem. Rev.* **1971**, *7*, 161−195.

(6) Manchanda, R.; Thorp, H. H.; Brudvig, G. W.; Crabtree, R. H. Proton-Coupled Electron Transfer in High-Valent Oxomanganese Dimers: Role of the Ancillary Ligands. *Inorg. Chem.* **1991**, *30*, 494−497.

(7) Petranovic, N.; Minic, D.; Sabo, T. J.; Dokovic, D. Kinetic and Thermodynamic Studies of Facial and Meridional *uns-cis*-[Co(eddp)-gly] Complexes. *J. Therm. Anal. Calorim.* **2000**, *59*, 807−814.

(8) Rehman, S.; Arshad, M.; Masud, K.; Afzal, R.; Salma, U. Pyrolytical Characterization of Transition Metal Complexes of Cobalt, Nickel, Copper and Zinc with Ethylene-diamine-*N*,*N*′-diacetate. *J. Therm. Anal. Calorim.* **2010**, *102*, 715−722.

(9) Kitamura, Y.; Shibata, A. Fluorine NMR Study of the Two cis-β-Configurations of a Hexafluoro-2,4-pentanedionatocobalt(III) Complex. *Polyhedron* **1992**, *11*, 2441−2446.

(10) Brothers, P. J.; Clark, G. R.; Palmer, H. R.; Ware, D. C. Condensation Reactions of Cobalt Amino Acid Complexes with Formaldehyde: Preparation and Crystal Structures of Cobalt Complexes Containing New Hexadentate, Pendant-Arm Macrocyclic and Acyclic Ligands. *Inorg. Chem.* **1997**, *36*, 5470−5477.

(11) Seng, H. L.; Ong, H. K. A.; Rahman, R. N. Z. R. A.; Yamin, B. M.; Tiekink, E. R. T.; Tan, K. W.; Maah, M. J.; Caracelli, I.; Ng, C. H. Factors Affecting Nucleolytic Efficiency of Some Ternary Metal Complexes with DNA Binding and Recognition Domains. Crystal and Molecular Structure of Zn(phen)(edda). *J. Inorg. Biochem.* **2008**, *102*, 1997−2011.

(12) Ng, C. H.; Ong, H. K. A.; Kong, C. W.; Tan, K. W.; Rahman, R. N. Z. R. A.; Yamin, B. M.; Ng, S. W. Factors Affecting the Nucleolytic Cleavage of DNA by (*N*,*N*′-Ethylenediamine-diacetato) metal(II) Complexes, M(edda). Crystal Structure of Co(edda). *Polyhedron* **2006**, *25*, 3118−3126.

(13) Ng, C. H.; Kong, K. C.; Von, S. T.; Balraj, P.; Jensen, P.; Thirthagiri, E.; Hamada, H.; Chikira, M. Synthesis, Characterization, DNA-binding Study and Anticancer Properties of Ternary Metal(II) Complexes of edda and an Intercalating Ligand. *Dalton Trans.* **2008**, 447−454.

(14) Kaluderovic, G. N.; Dinovic, V. M.; Juranic, Z. D.; Stanojkovic, T. P.; Sabo, T. J. Activity of Some Platinum(II/IV) Complexes with Edda-type Ligands against Human Adenocarcinoma HeLa Cells. *J. Coord. Chem.* **2006**, *59*, 815−819.

(15) Legg, J. I.; Cooke, D. W. The Stereochemistry of Some Cobalt(III) Complexes with Ethylenediamine-*N*,*N*′-diacetic Acid and Some *N*-Substituted Analogs. *Inorg. Chem.* **1965**, *4*, 1576−1584.

(16) Legg, J. I.; Cooke, D. W.; Douglas, R. E. Circular Dichroism of trans-*N*,*N*′-Ethylenediamine-diacetic Acid Cobalt(III) Complexes. *Inorg. Chem.* **1967**, *6*, 700−706.

(17) Legg, J. I.; Douglas, B. E. A General Method for Relating the Absolute Configurations of Octahedral Chelate Complexes. *J. Am. Chem. Soc.* **1966**, *88*, 2697−2699.

(18) Richardson, F. S. The Optical Activity of Dissymmetric Six-Coordinate Cobalt(III) Complexes. *Inorg. Chem.* **1972**, *11*, 2366−2378.

(19) Van Saun, C. W.; Douglas, B. E. Circular Dichroism of Cobalt(III) Complexes with Ethylenediamine-*N*,*N*′-diacetic Acid and a Carbonate, Oxalate, or Malonate Anion. *Inorg. Chem.* **1969**, *8*, 115−118.

(20) Jordan, W. T.; Legg, J. I. Correlation of Circular Dichroism and Stereochemistry in Cobalt(III) Chelates with Ethylenediamine-*N*,*N*′-diacetate. *Inorg. Chem.* **1974**, *13*, 955−959.
(21) Maricondi, C. W.; Douglas, B. E. Importance of Asymmetric Nitrogens to the Circular Dichroism of Alkyl-Substituted Ethylenediaminediacetic Acid Complexes of Cobalt(III). *Inorg. Chem.* **1972**, *11*, 688−691.
(22) Jordan, W. T.; Douglas, B. E. Circular Dichroism of Some Complexes of Cobalt(III) with Ethylenediaminediacetate and Related Ligands. *Inorg. Chem.* **1973**, *12*, 403−408.
(23) Maricondi, C. W.; Maricondi, C. Asymmetric Nitrogen Donors. A Critical Factor in Determining Rotational Strengths in Ethylenediaminepolyacetate-Cobalt(III) Complexes. *Inorg. Chem.* **1973**, *12*, 1524−1528.
(24) Marques, M. A. L.; Gross, E. K. U. Time-dependent Density Functional Theory. *Annu. Rev. Phys. Chem.* **2004**, *55*, 427−455.
(25) Wang, Y.; Wang, Y.; Wang, J.; Liu, Y.; Yang, Y. Theoretical Analysis of the Individual Contributions of Chiral Arrays to the Chiroptical Properties of Tris-diamine Ruthenium Chelates. *J. Am. Chem. Soc.* **2009**, *131*, 8839−8847.
(26) Gao, X.; Wang, Y.; Wang, Y.; Jia, J.; Su, X. Theoretical Analysis of the CD Spectra and Chiroptical Properties of $[M(bpy)_2(phen)]^{2+}$ and $[M(phen)_2(bpy)]^{2+}$ (M = Ru, Os) Chelates. *Sci. Sin. Chim.* **2011**, *41*, 1145−1155.
(27) Frisch, M. J.; Trucks, G. W.; Schlegel, H. B.; Scuseria, G. E.; Robb, M. A.; Cheeseman, J. R.; Scalmani, G.; Barone, V.; Mennucci, B.; Petersson, G. A.; et al.. *Gaussian 09*, revision A.02; Gaussian, Inc.: Wallingford, CT, 2009.
(28) Becke, A. D. Density-Functional Thermochemistry. III. The Role of Exact Exchange. *J. Chem. Phys.* **1993**, *98*, 5648−5652.
(29) Tomasi, J.; Mennucci, B.; Cammi, R. Quantum Mechanical Continuum Solvation Models. *Chem. Rev.* **2005**, *105*, 2999−3093.
(30) Ciofini, I.; Adamo, C. Accurate Evaluation of Valence and Low-Lying Rydberg States with Standard Time-Dependent Density Functional Theory. *J. Phys. Chem. A* **2007**, *111*, 5549−5556.
(31) Schäffer, C. E.; Bendix, J. Kohn-Sham DFT and Ligand-Field Theory − Is there a Synergy? *Can. J. Chem.* **2009**, *87*, 1302−1312.
(32) Figgis, B. N.; Hitchman, M. A. *Ligand Field Theory and Its Applications*; John Wiley and Sons Ltd.: New York, 2000.
(33) Rückamp, R.; Benckiser, E.; Haverkort, M. W.; Roth, H.; Lorenz, T.; Freimuth, A.; Jongen, L.; Möller, A.; Meyer, G.; Reutler, P.; et al. Optical Study of Orbital Excitations in Transition-metal Oxides. *New J. Phys.* **2005**, *7*, 144.
(34) Brown, A.; Kemp, C. M.; Mason, S. F. Electronic Absorption, Polarised Excitation, and Circular Dichroism Spectra of [5]-Helicene (Dibenzo[c,g]phenanthrene). *J. Chem. Soc. A* **1971**, 751−755.
(35) Hawkins, C. J. Vicinal and Conformational Contributions to the Circular Dichroism of Tetragonal Diaminecobalt(III) Complexes. *J. Chem. Soc. D* **1969**, 777−778.
(36) Wang, Y.; Fleischhauer, J.; Bausch, S.; Sebestian, M.; Laur, H. P. Conformational Analysis and TDDFT Calculations of the Chiroptical Properties of Tris[1,2-propanediolato(2^-)-κO,κO′] Selenium/Tellurium and Related Compounds. *Enantiomer* **2002**, *7*, 343−374.